

# Enhancement of surface plasmon polariton on graphene excited by four-wave mixing\*

ZHANG Yu-ping (张玉萍)\*\*, WU Zhi-xin (吴志心), ZHANG Hong-yan (张洪艳), XU Shi-lin (徐世林), ZHANG Xiao (张晓), LIU Ling-yu (刘陵玉), and ZHANG Hui-yun (张会云)

Key Laboratory of Terahertz Technology of Shandong Province, College of Science, Shandong University of Science and Technology, Qingdao 266590, China

(Received 14 June 2013)

©Tianjin University of Technology and Springer-Verlag Berlin Heidelberg 2013

We present a theoretical description of surface plasmon polariton (SPP) on a graphene surface excited by four-wave mixing using two laser beams. The phase-matched incident angles of the two beams that meet the SPP excitation conditions are calculated, and the discussion of the generated SPP power dependence on the incident angles is presented. We demonstrate that there is an enhancement in the peak power at the optimum angles at 633 nm and 921 nm, which is about 30 and 850 times larger than the corresponding peak power on a gold surface, respectively.

**Document code:** A **Article ID:** 1673-1905(2013)06-0458-3

**DOI** 10.1007/s11801-013-3105-4

Surface plasmon polaritons (SPPs) are transverse magnetic (TM)-polarized electromagnetic (EM) waves that are guided along metal-dielectric or dielectric-dielectric interfaces and decay exponentially in both media away from the interface. SPPs are limited in the vicinity of the interface, and the optical field enhancement occurs in specific nano-structures, such as nanospheres and nanoplatelets. As a guided wave, an SPP is not restricted by diffraction, and although absorption limits its propagation length to the submillimeter range, this guided wave is an ideal solution for subwavelength optics<sup>[1-4]</sup>.

The SPP properties are determined by the relative dielectric function of the surrounding media<sup>[3,5]</sup>. To experimentally realize the required phase matching, researchers usually use prism coupling with an attenuated total reflection technique or a diffraction grating (even plain roughness) on the metal surface<sup>[1-3,6,7]</sup>.

In the past few years, new methods of generating SPPs have been proposed<sup>[8,9]</sup>. Renger et al<sup>[8]</sup> reported the excitation of SPPs by nonlinear four-wave mixing (FWM), and Georges<sup>[1]</sup> presented the theory for the nonlinear SPP excitation on a metal surface by FWM, which leads to higher peak power. However, work published so far has not considered the excitation of SPPs by FWM on non-metal surfaces. Graphene, a nonmetal material, is suitable for photonic applications due to its unique photoelectric properties. A doped graphene sheet can bind surface plasmons with TM polarization provided that

$\text{Im}\sigma > 0$ <sup>[10]</sup>, where  $\sigma$  is the conductivity of the graphene, and it has been demonstrated that it is possible to obtain a positive  $\text{Im}\sigma$  in doped graphene<sup>[11]</sup>.

Based on the researches mentioned above, we propose a method of SPPs excited by FWM on a doped graphene surface as shown in Fig.1. A doped graphene sheet is placed on a SiO<sub>2</sub> substrate, the surface of which is irradiated with two laser beams with wavelengths of  $\lambda_1=707$  nm and  $\lambda_2=800$  nm. The incident angles measured from the surface normal in anti-clockwise direction are  $\theta_1$  and  $\theta_2$ , respectively, which are adjusted to satisfy the phase matching conditions between the FWM process  $\omega_4=2\omega_1-\omega_2$  (or  $\omega_4=2\omega_2-\omega_1$ ) with wave vector of  $k_4=2k_{1x}-k_{2x}$  (or  $k_4=2k_{2x}-k_{1x}$ ) and the SPPs on graphene surface. In this paper,  $\omega_4=2\omega_1-\omega_2$  and  $\omega_4=2\omega_2-\omega_1$  conditions are considered independently. For simplification, we ignore the nonlinear effects of the substrate.

Assuming that graphene sheet lies at  $z=0$ , the SiO<sub>2</sub> substrate is located in the region  $z<0$ , and the air is located in the region  $z>0$ . In the case of surface plasmon polariton on graphene excited by FWM, the nonlinear surface polarization at  $\omega_4$  can be written as  $\mathbf{P}_4^{(3)}(\mathbf{r}, t) = P_{4z,s}^{(3)}(x, t)\delta(z)\mathbf{z}$ <sup>[12]</sup>, which originates from the surface nonlinear third-order susceptibility tensor  $\chi^{(3)}$  with the irradiation of incident beams. Hence, in the plane-wave approximation, the nonlinear surface polarization related to the incident pump fields at  $\omega_4=2\omega_1-\omega_2$  can be expressed by

$$P_{4z,s}^{(3)}(x, t) = p_{4z,s}^{(3)} e^{i(\omega_4 t - k_4 x)}, \quad (1)$$

\* This work has been supported by the National Natural Science Foundation of China (No.61001018), the Natural Science Foundation of Shandong Province in China (Nos.ZR2011FM009 and ZR2012FM011), the Research Fund of Shandong University of Science and Technology (SDUST) in China (No.2010KYJQ103), the Project of Shandong Province Higher Educational Science and Technology Program (No.J11LG20), and the Science & Technology Project of Qingdao in Shandong Province in China (Nos.11-2-4-4-(8)-jch and 10-3-4-2-1-jch).

\*\* E-mail: sdust\_thz@yahoo.cn

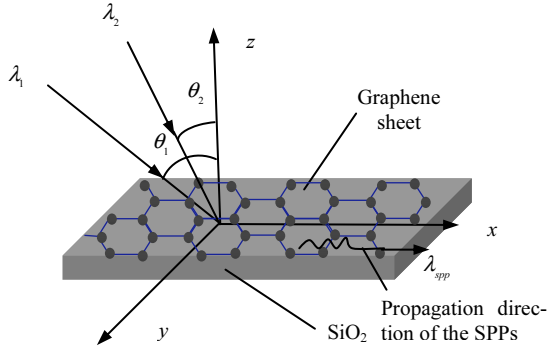


**Fig.1 Schematic diagram of the doped graphene on SiO<sub>2</sub>**

with

$$p_{4z,s}^{(3)} e^{i(\omega t - k_x x)} = \epsilon_0 \chi_s^{(3)} E_{1z} E_{2z}^* \quad (2)$$

where  $E_{1z} = (1 + \rho_1) \sin \theta_1 E_1$  and  $E_{2z} = (1 + \rho_2) \sin \theta_2 E_2$  are the  $z$  components of complex amplitudes of the electric fields at  $z=0_+$ , and  $\chi_s^{(3)}$  is the effective surface nonlinear susceptibility of graphene.  $\rho_i = [n(\omega_i) \cos \theta_i - \cos \theta_i] / [n(\omega_i) \cos \theta_i + \cos \theta_i]$ , ( $i=1,2$ ) are the Fresnel reflection coefficients, where  $n(\omega)$  and  $\theta_i$  are the complex index of refraction of graphene and the complex angle of refraction, respectively.

At  $z=0$ , a driven SPP can be generated by nonlinear polarization on graphene sheet, whose electric field can be expressed by<sup>[13]</sup>

$$E_4(x, y, z, t) = E_4(z) e^{i(k_x x - \omega_4 t)} \quad (3)$$

with

$$E_{4z} = \begin{cases} 2\pi i \left(\frac{\omega_4}{c}\right)^2 \frac{1}{\alpha_d} p_{4z,s}^{(3)} e^{-\alpha_d z}, & z > 0 \\ 2\pi i \left(\frac{\omega_4}{c}\right)^2 \frac{1}{\alpha_g} p_{4z,s}^{(3)} e^{-\alpha_g z}, & z = 0 \\ -2\pi i \left(\frac{\omega_4}{c}\right)^2 \frac{1}{\alpha_s} p_{4z,s}^{(3)} e^{\alpha_s z}, & z < 0 \end{cases} \quad (4)$$

where  $\alpha_d$ ,  $\alpha_g$  and  $\alpha_s$  present the  $z$  components of the wave vectors in air, graphene and SiO<sub>2</sub> substrate, respectively. Their relationships with dielectric constant of each medium are

$$\begin{cases} k_4^2 - \alpha_d^2 = (\omega_4 / c)^2 \epsilon_d \\ k_4^2 - \alpha_g^2 = (\omega_4 / c)^2 \epsilon_g \\ k_4^2 - \alpha_s^2 = (\omega_4 / c)^2 \epsilon_s \end{cases} \quad (5)$$

where  $\epsilon_d$ ,  $\epsilon_g$  and  $\epsilon_s$  are the relative permittivities of air, graphene and SiO<sub>2</sub> substrate, respectively. Furthermore, the relationship among  $H_{4y}$ ,  $E_{4x}$  and  $E_{4z}$  can be obtained from Maxwell's equations of this electric field, namely,

$$\begin{cases} i \frac{\omega_4}{c} H_{4y} = \frac{\partial E_{4x}}{\partial z} - i k_{spp} E_{4z} \\ \frac{\partial H_{4y}}{\partial z} = \frac{i \omega_4}{c} \epsilon_g E_{4x} \\ k_{spp} H_{4y} = -\frac{\omega_4}{c} \epsilon_g E_{4z} \end{cases} \quad (6)$$

where  $k_{spp} = k'_{spp} + i k''_{spp}$  is complex with  $k'_{spp}$  and  $k''_{spp}$  as the real and imaginary parts of SPP wave vector, respectively. The relation in Eq.(6) is also valid for air and SiO<sub>2</sub> substrate.

According to the boundary condition across the nonlinear polarization sheet, we can get

$$H_{4y} \Big|_{z=0^-} - H_{4y} \Big|_{z=0^+} = 4\pi \sigma(\omega_4) E_{4x}(0) \delta(z) / c \quad (7)$$

where  $\sigma(\omega_4) = \sigma^{\text{intra}}(\omega_4) + \sigma^{\text{inter}}(\omega_4)$  is the conductivity of graphene at  $\omega_4$  with<sup>[14]</sup>

$$\begin{cases} \sigma^{\text{intra}}(\omega_4) = \frac{2ie^2 T}{\pi \hbar (\omega_4 + i2\tau^{-1})} \left( -\frac{\mu}{K_B T} + 2 \ln \left( e^{-\frac{\mu}{K_B T}} + 1 \right) \right) \\ \sigma^{\text{inter}}(\omega_4) = \frac{ie^2}{4\pi \hbar} \ln \left[ \frac{2|\mu| - (\omega_4 + 2i\tau^{-1})\hbar}{2|\mu| + (\omega_4 + 2i\tau^{-1})\hbar} \right] \end{cases} \quad (8)$$

as the intra and inter conductivities of graphene, respectively. In Eq.(8),  $\mu$  is the chemical potential of graphene,  $\tau$  is the collision time, and  $T$  denotes the temperature.

Combining Eqs.(4)–(8), we obtain the dispersion relation for the SPP excitations in graphene surrounded by air and substrate as

$$\frac{\epsilon_s}{\sqrt{k_{spp}^2 - (\omega_4 / c)^2 \epsilon_s}} + \frac{\epsilon_d}{\sqrt{k_{spp}^2 - (\omega_4 / c)^2 \epsilon_d}} = \frac{4\pi}{i\omega_4} \sigma(\omega_4) \quad (9)$$

In each FWM process, one beam supplies two photons, and the other beam supplies a single photon. According to momentum conservation<sup>[15]</sup>, we have

$$k_4 = 2 \frac{\omega_1}{c} \sin \theta_1 - \frac{\omega_2}{c} \sin \theta_2 = k'_{spp} \quad (10)$$

In the same way,  $k_4$  at  $\omega_4 = 2\omega_2 - \omega_1$  can be described by

$$k_4 = 2 \frac{\omega_2}{c} \sin \theta_2 - \frac{\omega_1}{c} \sin \theta_1 = k'_{spp} \quad (11)$$

The curves in Fig.2(a) and (b) show the phase matching angles ( $\theta_1$ ,  $\theta_2$ ) that satisfy Eq.(10) in the cases of  $\omega_4 = 2\omega_1 - \omega_2$  and  $\omega_4 = 2\omega_2 - \omega_1$  with  $\lambda_1 = 707$  nm and  $\lambda_2 = 800$  nm, respectively. The circles on the curves indicate the optimum phase matching angles, which result in the maximum SPP power in the corresponding process.

Generally, the denotation  $I = c \epsilon_i^{1/2} |E|^2 / 2\pi$  is used to indicate the intensity of a plane wave in a medium with dielectric constant of  $\epsilon_i$ . So the power  $I_4$  of SPP generated by FWM can be represented as

$$I_4 = c \epsilon_g^{1/2} |E_4|^2 / 2\pi \quad (12)$$

where  $I_4 \propto I_2 I_1^2$  or  $I_4 \propto I_1 I_2^2$  with  $I_i = c \epsilon_i |E_i|^2$  ( $i=1, 2$ ) as the intensities of the two incident laser beams. As expressed in Eq.(12), under certain incident intensities, a higher  $I_4$  requires a larger value of  $\chi_s^{(3)}$  and the optimum phase matching angles ( $\theta_1$ ,  $\theta_2$ ) of two incident beams. For SPPs at the graphene-air interface, the absorption length defined as  $L_{spp} = 1 / (2k''_{spp})$  is much larger than the thickness of the nonlinearly polarized graphene surface layer. The effective surface nonlinear susceptibility of the graphene is about 37.5 times larger than that of gold<sup>[16,17]</sup>.

We calculate the SPP power  $I_4$  of each FWM process, and then normalize the values by the corresponding peak SPP power generated on a Au surface by FWM<sup>[1]</sup>. During the calculation, set  $\mu=45$  meV,  $\tau=2\times 10^{-13}$  s and  $T=300$  K, and the intensities of incident beams are identical to those of the beams incident on a gold surface in Ref.[1]. Compared with the SPPs generated on Au, there is a large enhancement in the SPP power from excitation on the graphene surface because of a larger real part of dielectric constant of graphene  $\epsilon_{g,r}$  and a higher effective surface nonlinear susceptibility  $\chi_s^{(3)}$  on graphene sheet. Fig.3 shows the dependence of the normalized power  $I_4$  on  $\theta_1$  for  $\lambda_4=633$  nm under the phase-matching conditions given in Fig.2. The peak SPP power occurs at  $(61.89^\circ, 32.10^\circ)$ , which are the optimum angles, and is about 30 times larger than that on the Au surface<sup>[1]</sup>. Optimization of the two angles of incidence is related to the factor of  $|(1+\rho_1)\sin\theta_1|^4|(1+\rho_2)\sin\theta_2|^2$ . At the peak of the power, the total z components of the laser electric fields are optimized, and the nonlinear surface polarization produced by FWM process reaches the maximum.

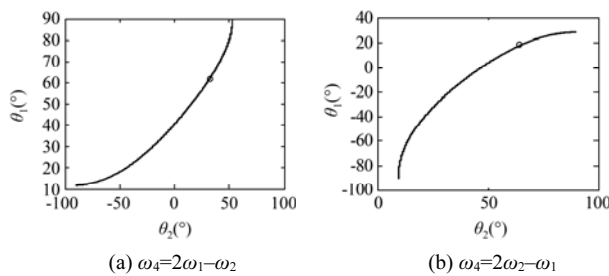


**Fig.2 Phase matching angles of incidence ( $\theta_1$ ,  $\theta_2$ ) in the cases of  $\omega_4=2\omega_1-\omega_2$  and  $\omega_4=2\omega_2-\omega_1$ , where the two circles represent the optimum phase matching angles**

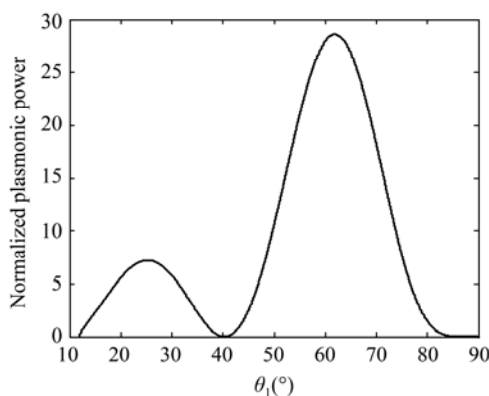


**Fig.3 Dependence of the normalized SPP power  $I_4$  on  $\theta_1$  for  $\lambda_4=633$  nm<sup>[1]</sup>**

Finally, Fig.4 shows the normalized  $I_4$  versus  $\theta_2$  under phase-matching conditions for  $\lambda_4=921$  nm. The peak SPP power occurs at  $(63.29^\circ, 19.15^\circ)$ , and is about 850 times larger than that on the Au surface<sup>[1]</sup>. Analogously, optimization of the two angles of incidence is related to the factor of  $|(1+\rho_2)\sin\theta_2|^4|(1+\rho_1)\sin\theta_1|^2$ .

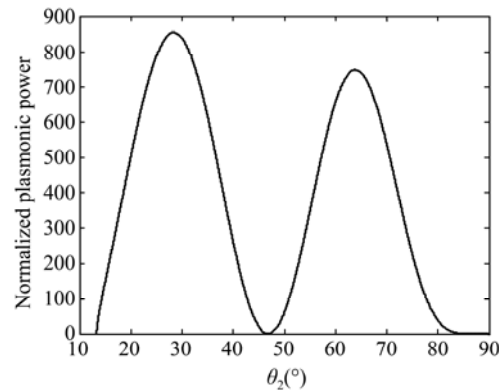


**Fig.4 Dependence of the normalized SPP power  $I_4$  on  $\theta_2$  for  $\lambda_4=921$  nm**

In summary, we present the theory for SPP on a graphene surface excited by FWM, and confirm an enhancement of the peak SPP power, which is about 1–3 orders of magnitude larger than the value on a gold surface reported in previous work. This work provides a theoretical foundation for future SPP applications.

**References**

- [1] A. T. Georges, J. Opt. Soc. Am. B **28**, 1603 (2011).
- [2] A. V. Zayats, I. I. Smolyaninov and A. A. Maradudin, Phys. Rep. **408**, 131 (2005).
- [3] Jie Su, Cheng Sun and Xiaoqiu Wang, Journal of Optoelectronics·Laser **24**, 408 (2013). (in Chinese)
- [4] Zhiqiang Hao, Jing Chen, Zongqiang Chen, Wenqiang Lu, Jingjun Xu and Qian Sun, Journal of Optoelectronics·Laser **23**, 1211 (2012). (in Chinese)
- [5] Rather H., Surface Plasmons on Smooth and Rough Surfaces and on Gratings, Springer-Verlag, 1988.
- [6] Yu. V. Bludov, M. I. Vasilevskiy and N. M. R. Peres, Euro. Phys. Lett. **92**, 68001 (2010).
- [7] Yu. V. Bludov, N. M. R. Peres and M. I. Vasilevskiy, Phys. Rev. B **85**, 245409 (2012).
- [8] J. Renger, R. Quidant, N. van Hulst, S. Palomba and L. Novotny, Phys. Rev. Lett. **103**, 266802 (2009).
- [9] N. E. Karatzas and A. T. Georges, J. Opt. Soc. Am. B **26**, 2218 (2009).
- [10] S. A. Mikhailov and K. Ziegler, Phys. Rev. Lett. **99**, 016803 (2007).
- [11] L. A. Falkovsky, J. Phys. **129**, 012004 (2008).
- [12] Y. R. Shen, The Principles of Nonlinear Optics, Wiley, 1984.
- [13] T. F. Heinz, H.-E. Ponath and G. I. Stegeman, Second-order Nonlinear Optical Effects at Surfaces and Interfaces, Elsevier, 1991.
- [14] George W. Hanson, J. Appl. Phys. **103**, 064302 (2008).
- [15] J. Renger, R. Quidant and L. Novotny, Opt. Express **19**, 1777 (2011).
- [16] E. Xenogiannopoulou, P. Aloukos, S. Couris, E. Kaminiska, A. Piotrowska and E. Dynowska, Opt. Commun. **275**, 217 (2007).
- [17] E. Hendry, P. J. Hale, J. Moger and A. K. Savchenko, Phys. Rev. Lett. **105**, 097401 (2010).